A Nanoindentation Based Study of Mechanical Properties of Al-Si-Cu-Mg Alloy Foam Cell Wall

Md Anwarul Hasan*, Amkee Kim†, Chang-Hun Lee*,
Hak-Joo Lee**, Soon-Gyu Ko** and Seong-Seock Cho***

나노인덴테이션에 의한 Al-Si-Cu-Mg 합금 폼 셀 벽의 기계적 물성 연구

하 산, 김엄기, 이창훈, 이학주, 고순규, 조성석

Key Words : Nanoindentation(나노인덴테이션), Metal foam(금속 폼), Mechanical properties (기계적 물성), Contact stiffness(접촉 강성)

Abstract

Nanoindentation technique has been used to measure the mechanical properties of aluminium alloy foam cell walls. Al-Si-Cu-Mg alloy foams of different compositions and different cell morphologies were produced using powder metallurgical method. Cell morphology of the foam was controlled during production by varying foaming time and temperature. Mechanical properties such as hardness and Young's modulus were calculated using two different methods: a continuous stiffness measurement (CSM) and an unloading stiffness measurement (USM) method. Experimental results showed that hardness and Young's modulus of Al-5%(wt.)Si-4%Cu-4%Mg (544 alloy) precursor and foam walls are higher than those of Al-3%Si-2%Cu-2%Mg (322 alloy) precursor and foam walls. It was noticed that mechanical properties of cell wall are different from those of precursor materials.

1. Introduction

Indentation experiments have been being performed for over 100 years to obtain hardness of materials [1], but the recent years have seen significant improvements in indentation equipments [1,2]. The most latest of them are the nanoindenter machines with which it is now possible to monitor both load and displacement of an indenter during indentation experiments with high precision and accuracy even in submicron range [3-5]. The technique more commonly known as nanoindentation technique has been widely being used now a days for measuring mechanical properties of thin films and surface layers [2,6]. A number of techniques have been developed towards the goal of evaluating the elastic modulus of thin films from nanoindentation load-displacement curve [7-9]. Attempts have also been made to get more intrinsic properties such as yield [1,10-13] or tensile strength [14] and even flow properties [15-20] from indentation tests.

So far the application of nanoindentation technique has been limited to thin films and surface layers but it can also be used for measuring the elastic and plastic properties of cell wall material of metal foams.

In this work we have used the nanoindentation technique to measure the mechanical properties of cell wall material of closed cell Al-alloy foams. The Al-Si-Cu-Mg alloy foams of different compositions were produced using powder metallurgical method. Hardness and elastic modulus of the precursors and foam walls were measured both from the unloading load-displacement curve and continuous stiffness measurement. The hardness and Young's modulus obtained from continuous stiffness measurement (CSM) method were higher than that otained from the

† 공주대학교 기계공학부
E-mail : amkee@kongju.ac.kr
TEL : (041)850-8616 FAX : (041)854-1449
* 공주대학교 기계공학과 대학원
** 한국기계연구원 기계구조그룹
*** 충남대학교 신소재공학부

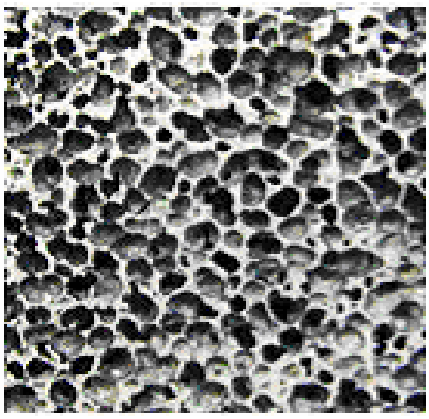

Fig. 1 Cellular structure of the produced Al-Si-Cu-Mg alloy.

unloading stiffness measurement (USM) method.

2. Experimental

2.1 Materials and specimens

The materials used in the study were Al-Si-Cu-Mg alloy foam of two different compositions namely alloy 322 (Al-3%Si-2%Cu-2%Mg) and alloy 544 (Al-5 wt% Si-4%Cu-4%Mg) foams. Both of the foams were produced using powder metallurgical method. Foam samples were obtained at different foaming time and different temperatures in the range 650 ^{o}C to 800 ^{o}C.

Specimens of 10 mm thickness were cut off from each of the foam samples and were mounted into thermo-set epoxy resin of 30 mm diameter x 15 mm thickness. One face of the mounted specimens was polished to mirror surface. While preparing the specimen, special care was taken so that after final polishing the opposite faces of the specimen are perfectly parallel to each other. A cellular structure of the alloy after foaming is shown in Fig.1.

2.2 Apparatus and indentation procedure

Experiments were performed using a Nanoindenter® XP a schematic illustration of which is shown in Fig. 2. At its most basic level the nanoindenter employs a high-resolution actuator to force an indenter into the test surface and a high-resolution sensor to continuously measure the resulting penetration. A diamond indenter is fixed to the end of the loading shaft that is suspended on delicate leaf springs. The leaf springs are compliant in the loading direction but stiff in the transverse direction. The movement of the indenter toward the sample is accomplished by varying the force supplied by the magnet-coil assembly while the displacement of the indenter is measured by a capacitance displacement gage. The system has load and displacement resolutions

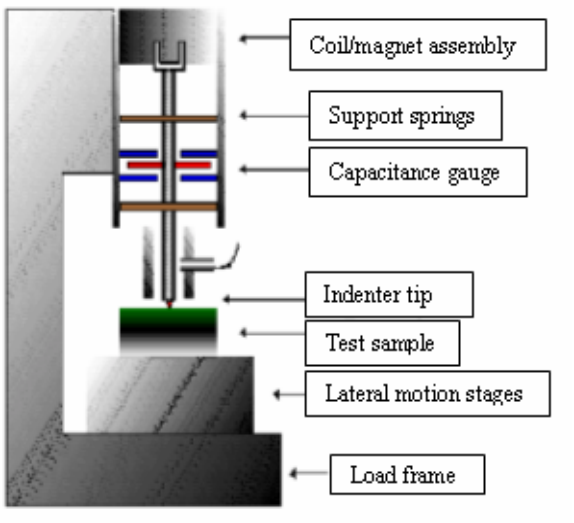

Fig. 2 A schematic representation of the experimental apparatus.

of 50 nN and 0.01 nm respectively while the maximum load and displacement that can be applied are 500 mN and 500 μm respectively. The indenter was a Berkovich indenter which is a three sided pyramid with an aspect ratio same as that of a Vickers indenter [22].

A total of 16 indentations were made in each of the specimen as shown in Fig. 3 and after analysis, result of those 16 indentations were averaged to obtain the mechanical properties of each of the specimen. It is suggested [21] that the successive indentations should be at least 20 times the maximum penetration depth when using the Berkovich indenter. The maximum penetration in our tests was 2000 nm, so we kept the distance between successive indentations to be 50 μm which is 25 times the maximum penetration.

2.3 Continuous stiffness measurement (CSM)

The contact stiffness between indenter and the specimen was continuously measured during indentation. The continuous measurement of stiffness was accomplished by applying a small oscillation to the force signal at a relatively high frequency (45 Hz). The amplitude of the force oscillation was 2 nm which is so small that the deformation process is not significantly affected by its addition. The corresponding displacement oscillation was monitored at the excitation frequency and the contact stiffness, S was calculated from the amplitude of the displacement signal. From this continuously measured stiffness the hardness and Young's modulus of the specimens were obtained continuously against the depth of indentation.

2.4 Unloading stiffness measurement (USM)

The unloading stiffness measurement is performed

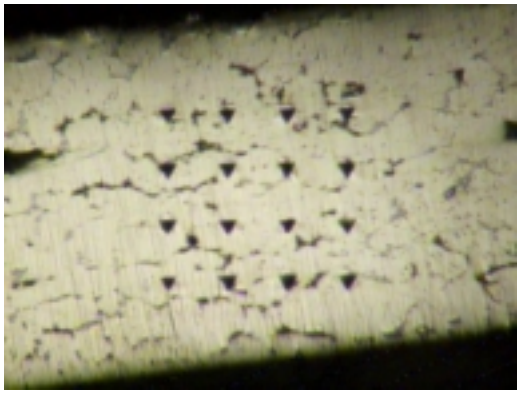

Fig. 3 Nanoindentation marks on the foam cell walls of alloy 322 foam, T = 800°C / t = 4.5 min

by obtaining a complete set of (both loading and unloading) load – displacement data and measuring the slope of the initial portion of the unloading curve, S = dp/dh. also known as the elastic stiffness of contact. From this elastic contact stiffness, it is possible to determine the hardness and elastic modulus of the material being tested. The equations used for this purpose are given by:

$$S = \frac{dp}{dh} = \frac{2}{\sqrt{\pi}} E_r \sqrt{A} \qquad (1)$$

$$\frac{1}{E_r} = \frac{1-\nu^2}{E} + \frac{1-\nu_i^2}{E_i} \qquad (2)$$

$$H = \frac{P}{A} \qquad (3)$$

Where S is the experimentally measured stiffness of contact, E_r is the reduced modulus (a parameter defined to account the effects of non rigid indenter on the load-displacement behavior) A is the projected area of elastic contact and β is a constant that depends only on the geometry of the indenter. The quantities E and υ are the Young's modulus and Poisson's ratio for the specimen, E_i and υ_i are the same parameters for the indenter, H is hardness, P is the applied load and A is the projected area of indentation. Incorporating the values of E_r (obtained from Eqn. 1), E_i, υ_i and υ in equation 2 gives the Young's modulus of elasticity of the material being tested while Eq. 3 gives the value of hardness.

3. Results and Discussion

Fig. 4 represents experimental load-displacement curves for alloy 322 foams. The indenter load was increased gradually starting from the surface of the specimen up to a maximum indenter tip displacement of 2000 nm. The load was then held constant for a period of 10 second. Peak load hold period in the load sequence diminishes the time dependent plastic effect and thus error caused by non elastic effect is minimized [8]. Peak load hold period also provides a means for accounting the thermal effect in terms of drift rate [21].

In the load displacement curve of Fig. 4. The differences in hardness of the materials are apparent from the difference in the peak load needed to attain maximum indentation. From the figure it is apparent that as the foaming time is increased at any foaming temperature, the load–displacement curve shifts upward indicating that a higher load is required for same indentation.

The Young's modulus of alloy 322 and alloy 544 precursors (material before foaming) are shown in Fig. 5 while the hardness of both precursors are shown in Fig. 6. It is evident from Figs. 5 and 6 that alloy 544

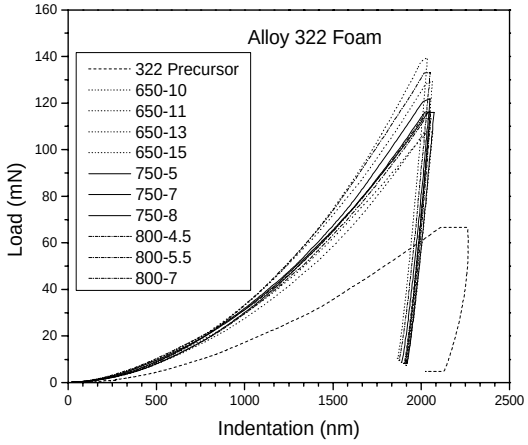

Fig. 4 The load-displacement curves of Alloy 322 foams obtained from nanoindentation test.

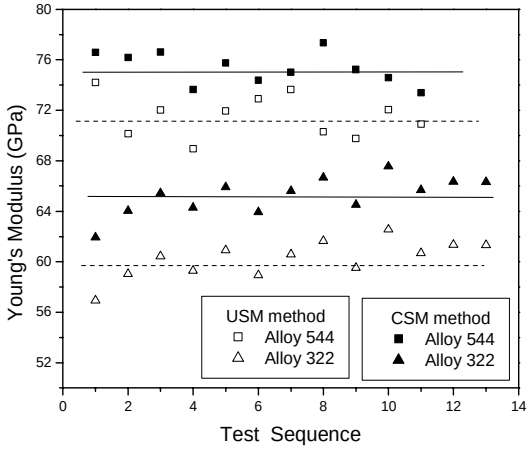

Fig. 5 Young's modulus of Al-Si-Cu-Mg alloys before foaming

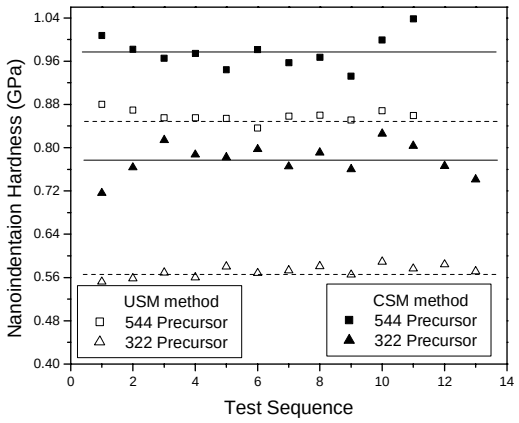

Fig. 6 Nanoindentation hardness of the Al-Si-Cu-Mg alloys before foaming

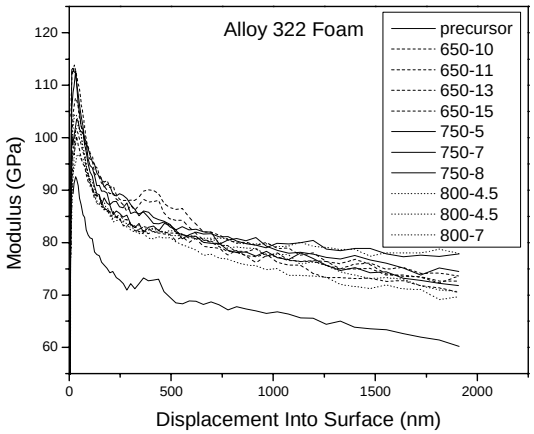

Fig. 7 The Young's modulus versus displacement curves of precursor and foam cell walls of Alloy 322 specimens obtained from CSM method.

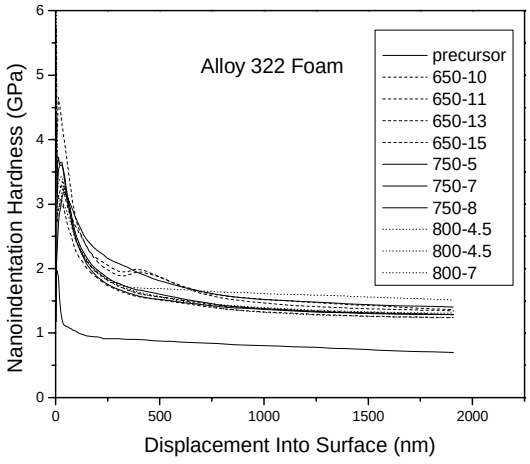

Fig. 8 The hardness versus displacement curves of precursors and foam cell walls of Alloy 322 specimens obtained from CSM method.

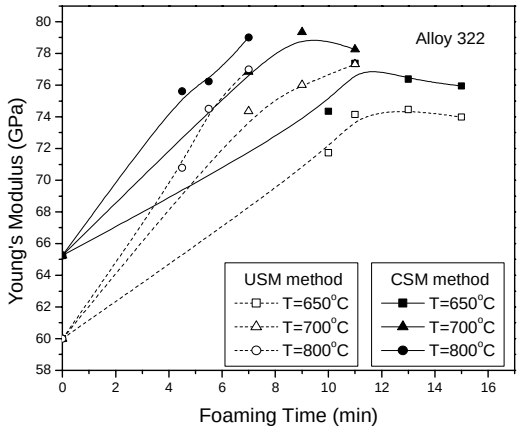

(a)

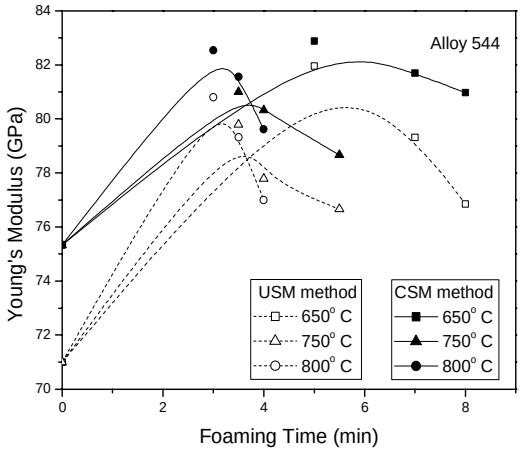

(b)

Fig. 9 The Young's modulus versus foaming time curves of foam cell walls (a) Alloy 322 specimens (b) Alloy 544 specimens.

precursor has higher Young's modulus and hardness than alloy 322 precursor. The higher hardness and Young's modulus of alloy 544 precursor is associated with the higher alloying element effect in 544 alloy.

Fig. 7 represents the Young's modulus versus indentation curves of alloy 322 foam cell walls which were obtained from continuous stiffness measurement method. All of the curves showed that Young's modulus of the cell walls changes with indentation depth. Initially the value of Young's modulus rises sharply and reaches a very high value. As the indenter penetrates into the specimen, the value of Young's modulus decreases gradually finally reaching a nearly constant value after a certain depth.

We accepted the average Young's modulus in the range 1000 nm to 1500 nm indentation depth as the Young's modulus of the specimens because in this range the Young's modulus and hardness showed minimum sensitivity to the indentation depth.

Fig. 8 represents the nanoindentation hardness versus indentation curves of alloy 322 precursor and foam cell walls obtained from continuous stiffness measurement method. The hardness of precursors and foam specimens also presented a similar trend as Young's modulus with respect to indentation depth, with a clear evidence that nanoindentation hardness value depends on the indentation depth. The Young's modulus (Fig. 7) and the hardness value (Fig. 8) of specimens decreased as indentation depth increased, with the decrease being more pronounced at low indentation depth. This is due to the reason that the penetration depth is obtained by considering the shape of the indenter tip to be an ideal triangular pyramid, but the real indenter tip is slightly spherical [22].

Although at sufficiently high load the tip radius in comparison to indentation depth is negligible, when the penetration depth of the indenter is very small the effect of the radius of this spherical tip is not negligible. Thus recorded indentation depth is lower than the real penetration and hence hardness value is much high.

The sharply rising initial portion of Young's modulus-displacement and hardness-displacement curves is a reflection of the surface roughness of the specimen [23]

The variations of Young's modulus of 322 and 544 specimens with respect to foaming time period are shown in Figs. 9 (a) and (b) respectively while the variations of hardness with respect to foaming time and temperature are shown in Figs. 10 (a) and (b). In these figures, remarkable increase in Young's modulus and hardness value is observed with increase of foaming time period at all foaming temperatures. A comparison of Young's modulus and hardness of the precursors and foam walls obtained from the unloading stiffness meth (USM) analysis and continuous stiffness measurement (CSM) method reveal that the result from CSM method is always higher than that obtained from USM method.

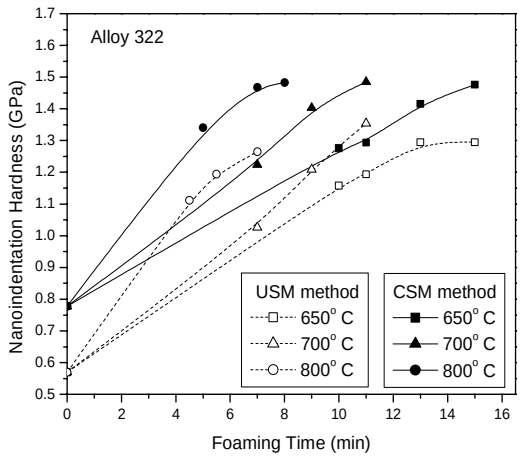

(a)

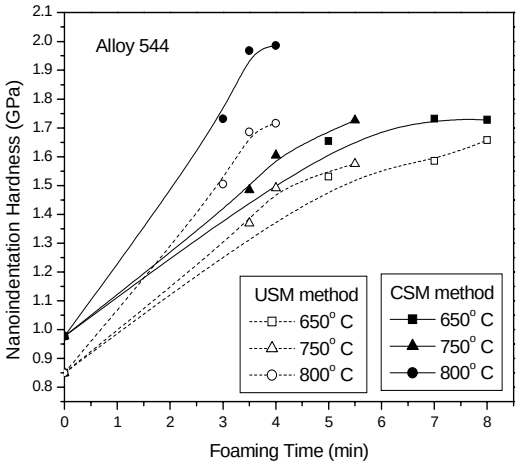

(b)

Fig. 10 The foaming time versus nanoindentation hardness curves of foam cell walls (a) Alloy 322 specimens (b) Alloy 544 specimens

4. Conclusions

Nanoindentation tests were conducted to verify the applicability of nanoindentation method for measuring material properties of foam cell walls and to characterize the mechanical properties of Al-Si-Cu-Mg-TiH_2 alloy foam cell walls of two different compositions. The following results can be summarized:

1. The hardness and Young's modulus of specimens decrease with increasing indentation depth, and tend to converge at sufficiently high loads. An average result in the range 1000nm to 1500nm was considered to be the representative data for the specimens in case of CSM method.

2. Alloy 544 precursor and foam cell wall showed higher hardness and elastic modulus than alloy 322 precursor and foam cell wall regardless of measurement method.

3. The elastic modulus and hardness obtained from continuous stiffness measurement are higher than those obtained from unloading load displacement curve analysis i.e. unloading stiffness measurement method.

4. Both Young's modulus and hardness increased with increase of foaming time which indicates that the mechanical properties of foam cell walls are not exactly same as those of the precursor materials from which foams are made.

Acknowledgement

This research was sponsored by the Korea Science and Engineering Foundation (KOSEF) under contract No. R01-2002-000-00093-0(2002) from its basic

research program. The authors of this paper wish to acknowledge the financial support of KOSEF for this work.

References

(1) D. Tabor, 1996, The Hardness of Metals, (Oxford, London, 1951); Phil. Mag. Vol. A74, pp. 1207
(2) W.D. Nix, 1988, "Mechanical Properties of Thin Films", *Met. Trans.,* A, Vol. 20A, pp. 2217-2244
(3) J. B. Pethica, R. Hutchings and W.C. Oliver, 1983, *Phil. Mag*., Vol. A48, pp. 593
(4) D. Stone, W. R. KaFibtaube, P.Alexopoulos, T. W. Wu, and C. Y. Li, 1988, *J.Mater. Res*. Vol. 3, pp. 141
(5) B. Bhushan, A. Kolkarmi, W. Bonin and J. Wyrobek, 1996, *Phel. Mag.* Vol. A74, pp. 1117
(6) Min Li, Manual L. Palacio, C. Barry Carter, and William W. Gerberich, 2002, "Indentation deformation and fracture of thin polystyrene films", *Thin Solid Films*. Vol. 416, pp. 174-183.
(7) M. F. Doerner and W. D. Nix, 1986, *J. Mater. Res*. 1, pp. 601
(8) W. C. Oliver and G. M. Pharr, 1992, *J. Mater. Res.* Vol. 7, pp. 1564
(9) W.W. Gerberich, W. Yu, D. Kramer, A. Stronjny, D. Bahr, E. Kukkeidden and J. Nelson, 1998, *J. Mater. Res.* Vol. 13, pp. 421
(10) D.M. March, 1964, Proc. R. Soc. London, Vol. A 279, pp. 420
(11) C. H. Mok, 1966, Exp. Mech. Feb, pp. 87
(12) R.A. George, S. Dinda, A.S. Kasper, 1976, Met. Progr. May 30
(13) D. Kramer, H. Huang, M. Kriese, J. Robach, J. Nelson, A. Wright, D. Bahr, W.W. Gerberich, 1933, *Acta Mater.,* Vol. 47 (1), pp. 333
(14) J. H. Underwood, G.P. O'Hara, J. J. Zalinka, 19876, Exp. Mech. Dec., pp. 379
(15) H. A. Francis, 1976, Trans. ASME (Series H), Vol. 9 pp. 272
(16) F. M. Haggag, W. R. Corwin, W.L. Server (Eds.), 1993, ASTM STP 1204, American Society for Testing and Materials, Philadelphia, pp.27-44
(17) J. S. Field, M. V. Swain, 1995, *J. Mater. Res*., Vol. 10 (1), pp. 101
(18) A. C. Fischer-Cripps, B. R. Lawn, 1996, *Acta Mater.,* Vol. 44 (2), pp. 519
(19) J. Alcala, A.E. Giannakopoulos, S. Suresh, 1998, *J. Mater. Res.*, Vol. 13 (5), pp. 1390
(20) B. Talijat, T. Zacharia, F. Kosel, 1998, *Int. J. Solids Struct.*, Vol. 35 (33), pp. 4411
(21) Nanoindentation XP User's manual (version.16), pp.32,
(22) H. Ishikawa, S. Fudetani, M. Hiroshashi, 2001, *Applied Surface Science*, Vol. 178, pp. 56-62
(23) D. H. Kim, J. K. Kim, M. L. Sharm and P. Hwang, 1998, *Metals and Materials*., Vol. 4, No. 4, pp. 812-817